www.czasopisma.pan.pl PAN POLSKA AKADEMIA NAUK www.journals.pan.pl

Arch. Metall. Mater. **64** (2019), 2, 617-622

DOI: 10.24425/amm.2019.127588

YEON-JI KANG*, JONG-HO KIM**, JONG-IL HWANG***, KEE-AHN LEE*#

EFFECT OF T6 HEAT TREATMENT ON THE SCRATCH WEAR BEHAVIOR OF EXTRUDED Al-12WT.%Si ALLOY

This study investigated the effect of T6 heat treatment on the microstructure and scratch wear behavior of hypoeutectic Al-12wt.%Si alloy manufactured by extrusion. Microstructural observation identified spherical eutectic Si phases before and after the heat treatment of alloys (F, T6). Phase analysis confirmed Al matrix and Si phase as well as Al_2Cu and Al_3Ni, Mg_2Si in both alloys. In particular, Al_2Cu was finer and more evenly distributed in T6 alloy. This resulted in Vickers hardness of T6 alloy that was 2.3 times greater compared to F alloy. The scratch wear test was conducted using constant load scratch test (CLST) mode and multi-pass scratch test (MPST) mode. The scratch coefficient and worn out volume obtained by such were used to evaluate wear properties before and after heat treatment. In the case of T6 alloy, its scratch coefficient was lower than F alloy in all load ranges. After 15 repeated tests to measure worn out volume, F alloy and T6 alloy measured 1.2×10^{-1} mm^3 and 7.8×10^{-2} mm^3, respectively. In other words, the wear resistance of T6 alloy were confirmed to be better than those of F alloy. In addition, this study attempted to identify the microstructural factors that contribute to the better scratch wear resistance of T6 alloy and wear mechanism from surface and cross-section observations after the wear tests.

Keywords: Al-12wt.%Si alloy, Scratch test, Wear-resistance, T6 heat treatment

1. Introduction

Al-12% Si alloy has semi-metallic silicon particles on light-weight aluminum matrix which are distributed like a composite structure. So it has excellent lightness, superior wear resistance, high formability, low thermal expansion, and high corrosion resistance [1-3]. Applying hot extrusion to Al-12%Si alloy can improve the mechanical properties of the alloy. As hot extrusion is applied, the grain size decreases and equiaxed grains are formed by dynamic recrystallization. In addition, it is reported that the extrusion spherialize the Si phase and reduce its size, and also achieves even distribution of Si in an Al matrix [4]. In Al-Si based alloys, heat treatment for precipitation hardening can effectively control mechanical properties. Applying T6 heat treatment to Al-12wt.%Si with Mg and Cu elements added can improve strength and hardness properties due to $\beta''(Mg_2Si)$ and $\theta''(Al_2Cu)$ precipitates formed within the matrix [5-7].

There have recently been attempts to analyze the wear properties of materials using scratch tests [8,9]. A scratch wear test is a relatively simple method and can be applied to small specimens, and it is also known to be able to attain reliable outcomes from abrasive wear, which comprises more than 50% of all damage to regular materials caused by wear [10-15]. A scratch wear test using a diamond pin is particularly useful in interpreting and understanding wear behaviors in severe abrasive wear environments.

Multiple studies of the microstructure and properties of Al-Si-based alloys have been implemented. However, most of the studies focused on the processes controlling the shape and size of Si phases in Al-Si alloys. At present, there are few studies that investigate the effect of T6 heat treatment and wear mechanism of abrasive wear, the main wear mode of Al-Si-based alloy.

This study used a scratch wear test to evaluate the wear properties of Al-12wt.%Si manufactured by the extrusion process, and investigated the effect T6 heat treatment on microstructure and wear behavior.

2. Experimental

Al-12wt.%Si alloy used in this study was manufactured with hot extrusion at a 17.7:1 extrusion ratio after homogenization heat treatment. The specimen with a plate shape of 50 mm in width and 15 mm in thickness were prepared. The hot extrusion process was implemented at a billet temperature of 370°C and ram speed of 1.7 mm/s. The results of inductively coupled plasma (ICP) analysis (wt.%) were obtained as Al-12.19%Si-1.03%Cu-0.97%Ni-0.67%Mg-0.15%Fe. The extruded Al-12%Si

* INHA UNIVERSITY, DEPARTMENT OF MATERIALS SCIENCE AND ENGINEERING, INCHEON 22212, REPUBLIC OF KOREA
** RESEARCH INSTITUTE OF INDUSTRIALS SCIENCE & TECHNOLOGY, POHANG 37673, REPUBLIC OF KOREA
*** LIGHT METAL SOLUTION CO., LTD, YESAN 32446, REPUBLIC OF KOREA
# Corresponding author: keeahn@inha.ac.kr

was then solid solution heat treated at 510°C for 10 hrs, and underwent further aging at 175°C for 10 hrs. The specimen was etched using modified Keller's solution (2ml HF, 3ml HCl, 20ml HNO_3, distilled water 175 ml). Microstructural observations were made using a field emission scanning electron microscope (FE-SEM), electron probe X-ray micro analyzer (EPMA) and electron backscatter diffraction (EBSD). For hardness evaluation, each specimen was tested 12 times using a Vickers hardness tester and the average was calculated. A scratch wear test was implemented using RB311 scratch equipment with a 120° diamond tip at room temperature/humidity non-lubricated (dry) condition. At that time, a single scratch wear method with the constant load scratch test (CLST) and a multi-pass scratch test (MPST) method repeated in a single location were performed. The CLST test was tested at each load ranging from 0.5 kgf to 3.5 kgf by 0.5 kgf units. The MPST was implemented 15 times at 0.5 kgf. From the data obtained, the normal force (F_N) / tangential force (F_T) value, so called scratch coefficient of friction (SCOF), was calculated. Furthermore, the cross section of the wear area was observed after the scratch test to measure and calculate the worn out volume. SEM was used to observe the wear area and examine the wear behavior.

3. Results and discussion

The microstructural observation and phase analysis results before and after heat treatment are presented in Fig. 1. The grain size of F alloy and T6 alloy measured with low-magnification FE-SEM observation was 8.9 μm and 12.6 μm on average,

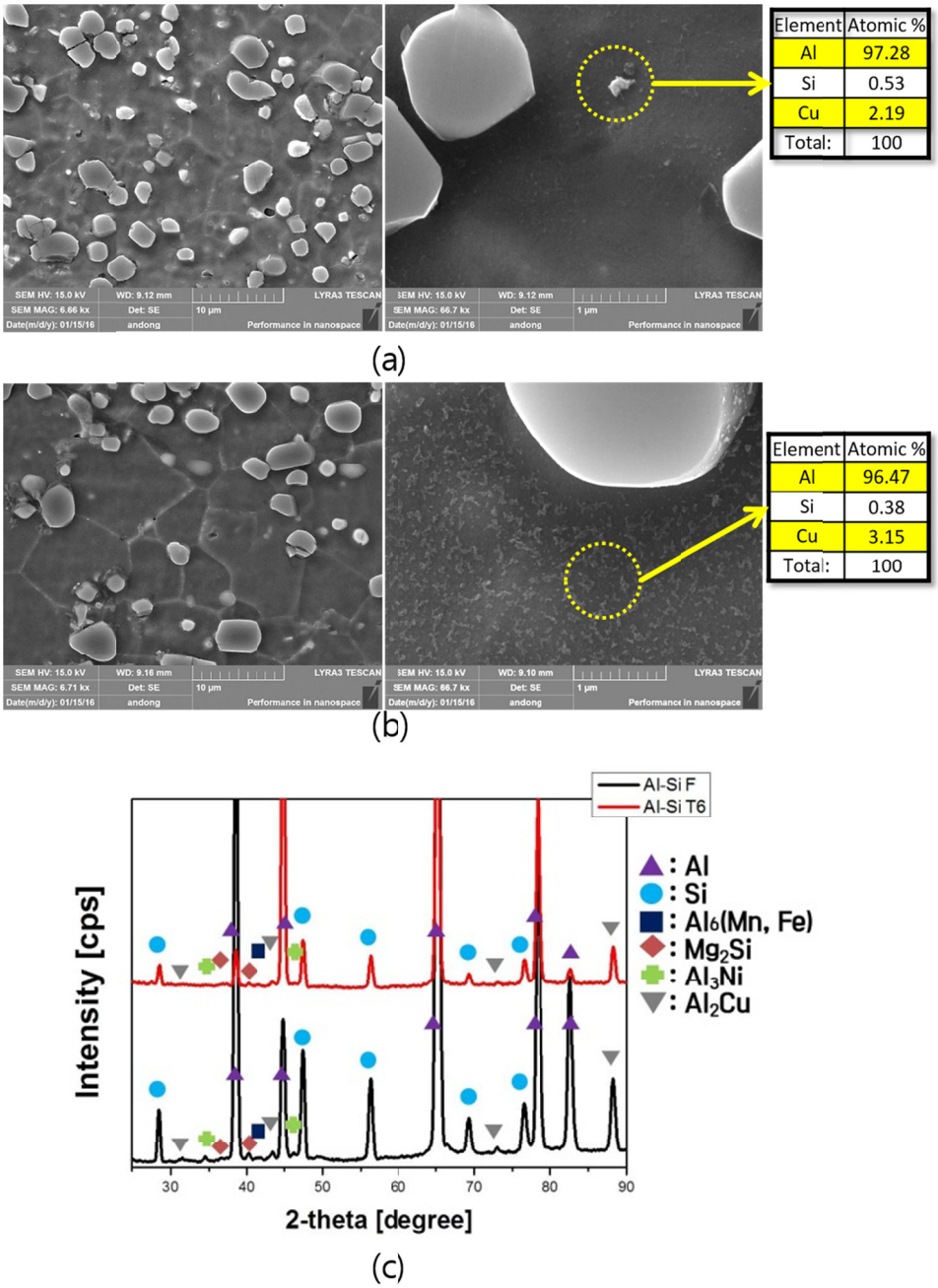

Fig. 1. SEM microstructures of extruded Al-12wt.%Si alloys ((a) F alloy, (b) T6 alloy) and (c) X-ray diffraction analysis results of those alloys

respectively. In the case of eutectic Si phase, it was identified as spherical in both alloys [4]. Si size increased slightly as heat treatment was applied, from approximately 2.3 μm to 2.8 μm, but the ratio decreased slightly. XRD phase analysis results (c) showed that main phase Al and eutectic Si phase as well as Al_2Cu, Al_3Ni, Mg_2Si and $Al_6(Mn, Fe)$ phases were present in both (F, T6) alloys. High-magnification FE-SEM observation results identified Al_2Cu (θ'') phase in the matrixes of both alloys. However, in F alloy (Fig. 1 (a), right) the Al_2Cu (θ'') phase was relatively massive and uneven, while in T6 alloy ((b), right) the θ'' phase was finer and evenly distributed. This is contributed by the fine re-precipitation of θ'' phase during artificial aging after solution heat treatment (510°C).

The hardness of extruded Al-12wt.%Si alloy measured in the normal direction (ND) was 54.8 Hv and in the extruded direction (ED) was 56.0 Hv in F alloy, and ND: 123.9 Hv and ED: 125.0 Hv in T6 alloy. Despite the grain size having increased after T6 heat treatment, the hardness of T6 alloy increased about 2.2 times.

EBSD analysis results in Fig. 2 show F alloy (a) to feature similar grain orientations, but T6 alloy (b) to feature grains that are recrystallized and grew in various orientations. As shown in the area outlined in black dotted square in Fig. 2(b), distribution of multiple fine misfits (low angle boundary) was observed. This can be understood to be contributed by the fine re-precipitation (T6 alloy) of θ'' phase (Fig. 1(b)) observed in the FE-SEM observation results. This is also suspected to be the main cause of the increased hardness properties of T6 alloy. In addition, the area outlined in yellow square in Fig. 2(b) shows evidence of lattice distortion in the eutectic Si phase and matrix after T6 heat treatment. This is reported to be due to the difference in thermal expansion coefficient between the Al matrix and the Si semi-metal particles [16]. The thermal expansion coefficient of Al matrix and Si phase are 7.63×10^{-6} and 28.7×10^{-6}, respectively, which is a difference of approximately 3.8 times. As a result, during quenching after solution heat treatment, a compressive stress field was formed on the Al matrix around the Si phase [16-18]. This also is suspected to be an additional factor that contributes to the increased hardness of Al-12wt.%Si T6 alloy.

Fig. 3 shows the scratch wear properties, scratch coefficient (a) and worn out volume (b) of Al-12%Si alloys (F, T6) in each load. The coefficients of T6 alloy measured lower than F alloy in all loads from 0.5 kgf to 3.5 kgf range. As shown in Fig. 3(b), the loss volume of the worn area increased according to load increase in both alloys regardless of heat treatment. The figure also confirms that the worn out volume of T6 alloy is significantly lower (greater wear resistance) compared to F alloy regardless of load condition.

Fig. 4 shows the wear properties according to the number of repeated scratches at 1 kgf load condition. Fig. 4(a) and (b) are graphs comparing the scratch coefficient of F alloy and T6 alloy

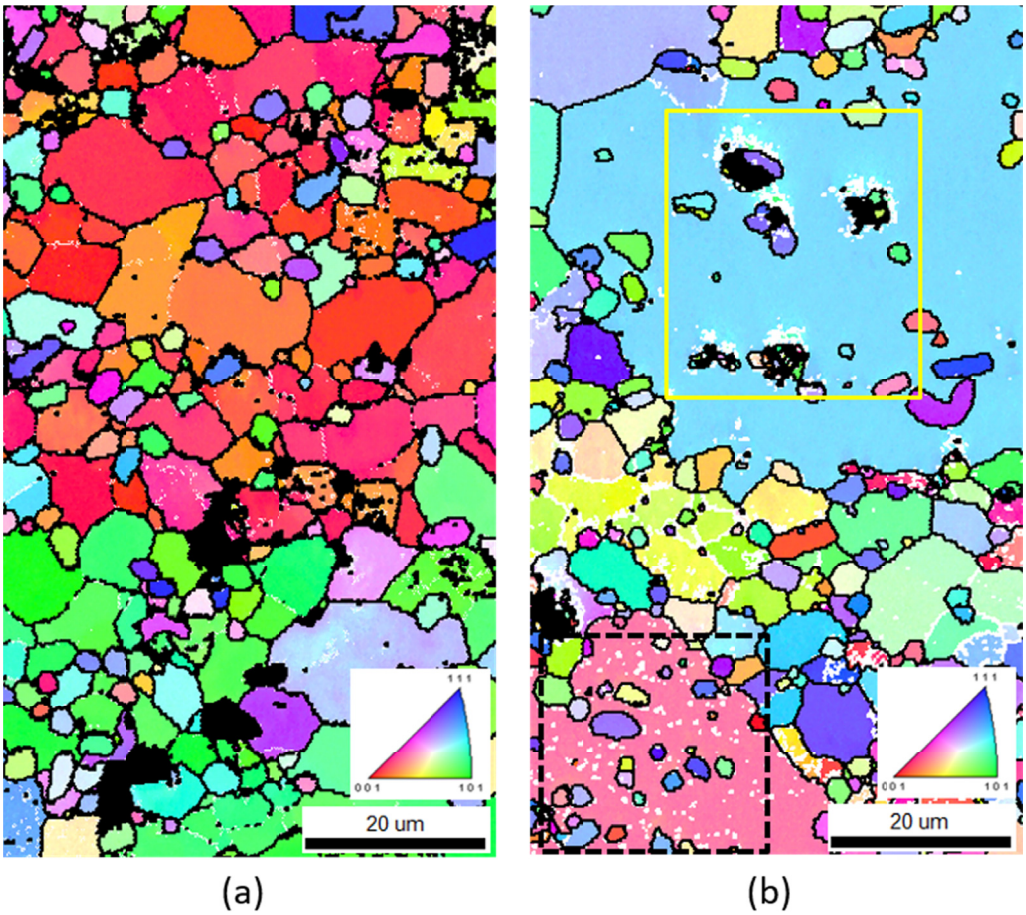

Fig. 2. EBSD analysis results of extruded Al-12wt.%Si alloys; (a) F alloy and (b) T6 alloy

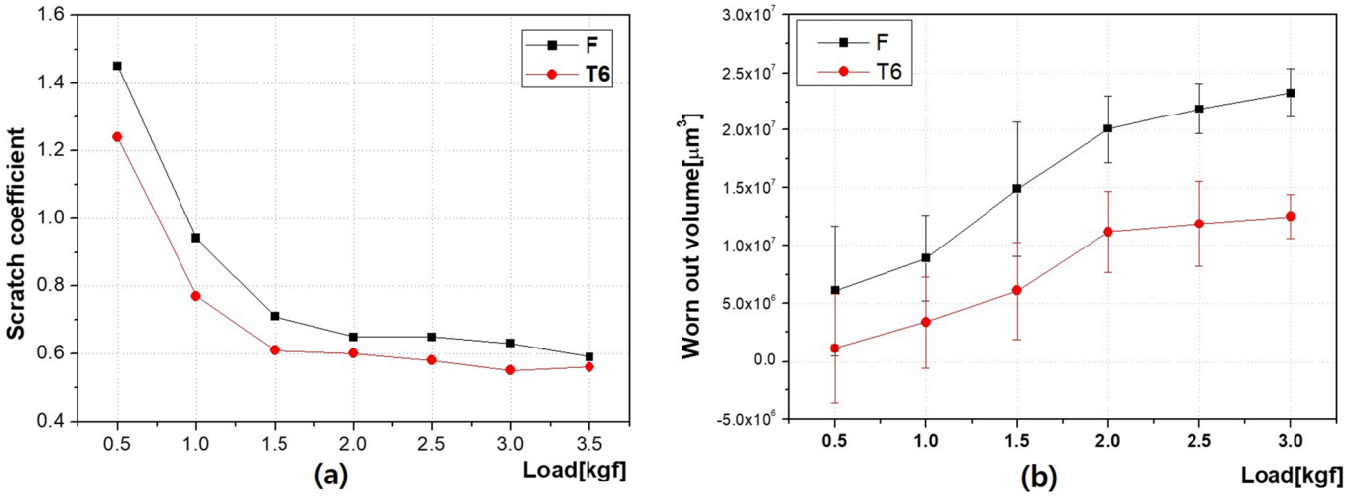

Fig. 3. Scratch wear properties with increasing load of extruded Al-12wt.%Si F, T6 alloys; (a) scratch coefficient and (b) worn out volume

obtained from one scratch (a) and 15 scratches (b). In F alloy, the coefficient decreased by 0.35 from 1.59 at one scratch to 1.24 at 15 scratches. In T6 alloy, the coefficient decreased by 0.24 from 1.29 at one scratch to 1.05 at 15 scratches. Furthermore, T6 alloy has a lower coefficient compared to those of F alloy. As the number of scratch tests increased, the coefficient reduction was relatively small in the T6 alloy and the deviation also decreased. Fig. 4(c) shows the worn out volume with increasing the number of scratch tests, and the wear volume of 15 times repeated scratches measured 1.2×10^{-1} mm^3 in F alloy and 7.8×10^{-2} mm^3

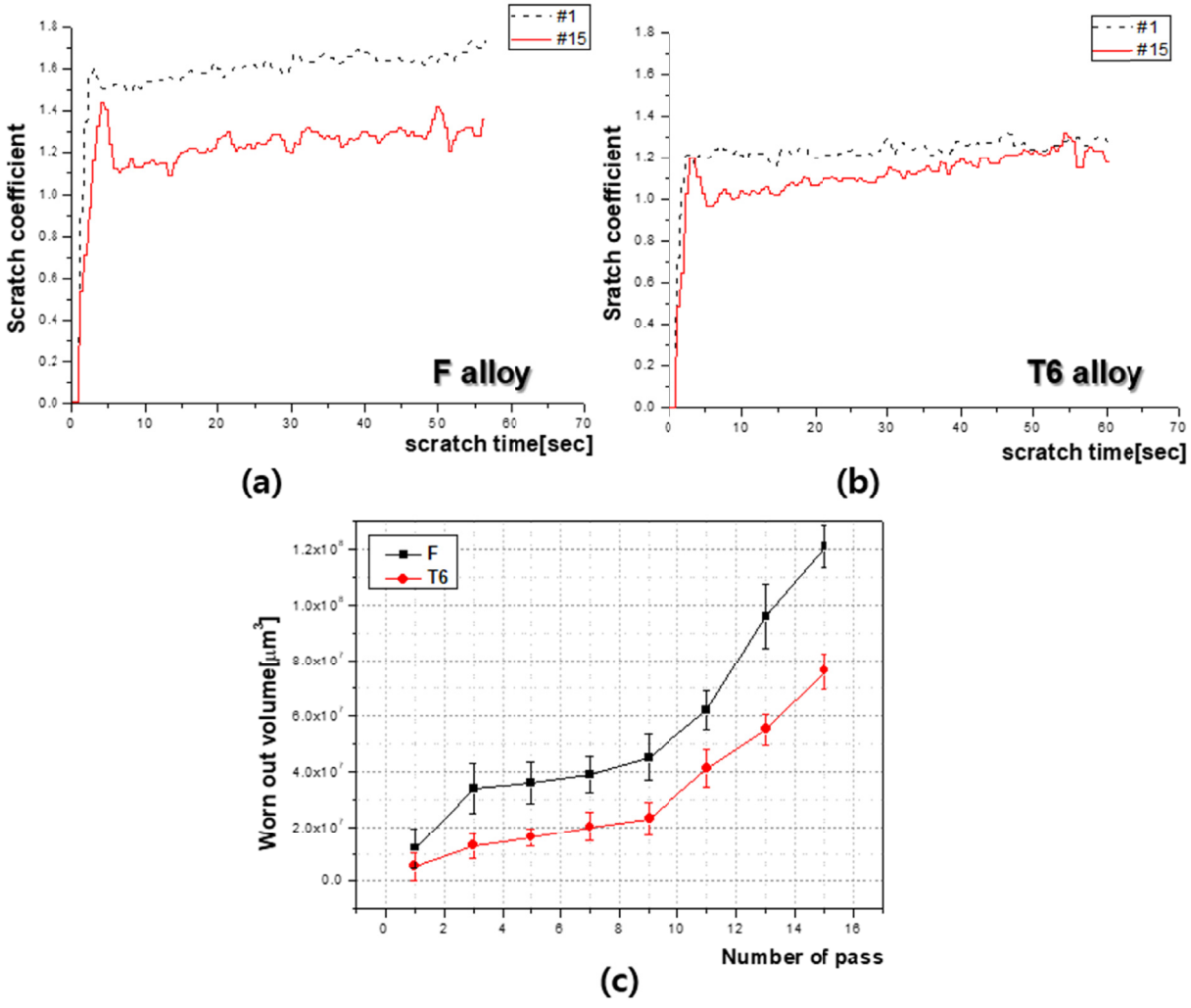

Fig. 4. Scratch wear properties with increasing number of pass (a) scratch coefficient of F alloy, (b) scratch coefficient of T6 alloy and (c) worn out volume

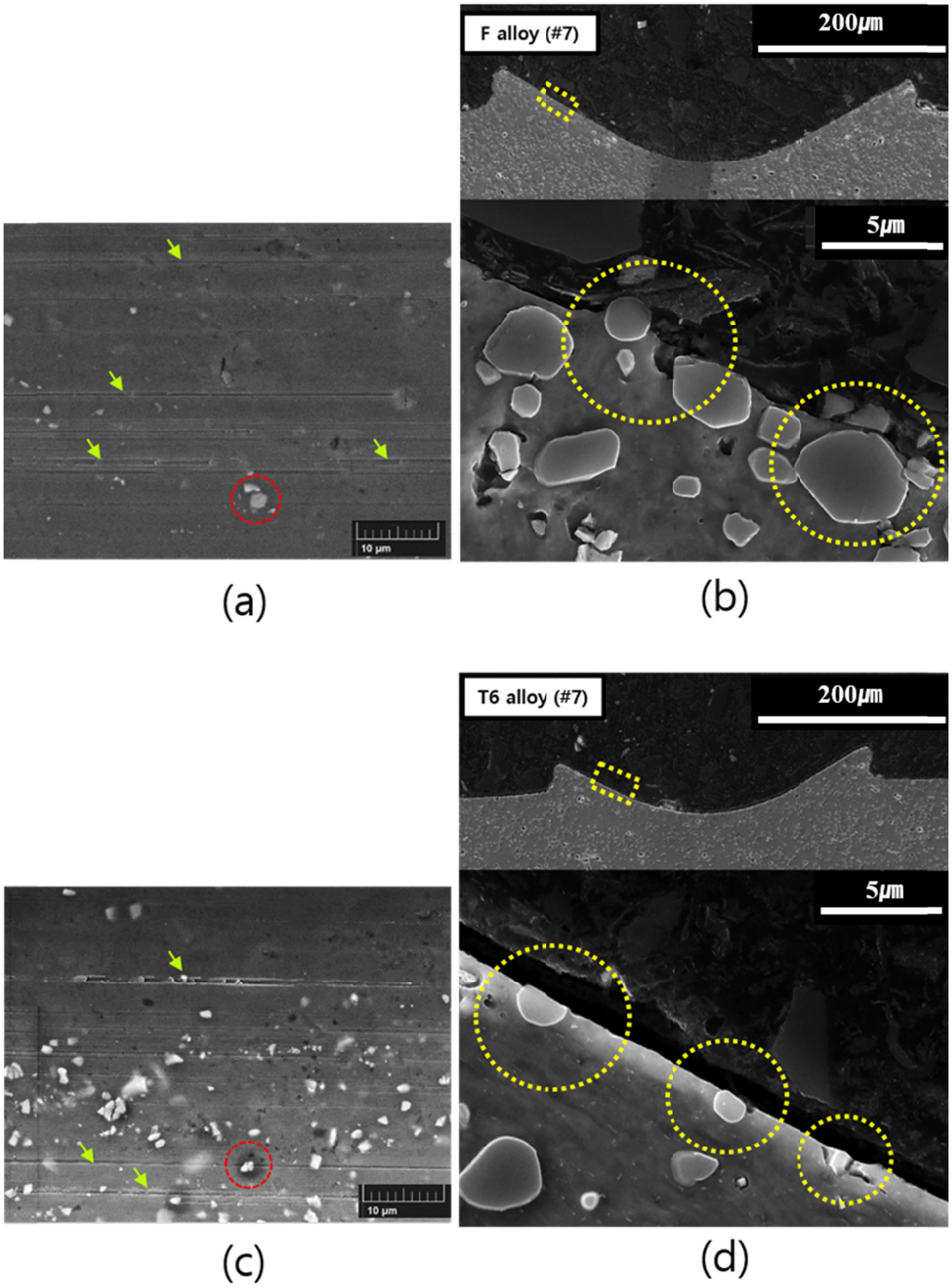

Fig. 5. Deformed microstructure after scratch wear tests. Worn out surfaces and cross-section areas of (a),(b) F alloy and (c),(d) T6 alloy

in T6 alloy. In other words, the worn out volume of T6 alloy is significantly lower than F alloy, which results in another evidence of the greater scratch wear resistance of T6 alloy. Based on the above results, it is assumed in the F alloy that the diamond tip experienced more abrasion with the Si phase than the T6 alloy as the diamond tip with the load is pressed in deeper. On the other hand, T6 alloy is assumed to have achieved greater wear resistance due to the reinforced matrix formed by age hardening and the smaller hardness difference between reinforced Si phase and matrix.

Fig. 5 is the SEM observation results of wear surfaces (a, c) and cross sections (b, d) after scratch wear tests. On the wear surfaces of both F and T6 alloys, typical abrasive wear behavior with micro-plowing ((a), (c) circled in red) and three-body abrasion wear tracks (marked by arrows) were observed. The high-magnification observation of the cross section of F alloy's wear surface (Fig. 5(b)) represented local defects at the interface between Si phase and matrix, and further identified Si particle's dislocating. On the other hand, observations of the cross section of T6 alloy's wear surface (Fig. 5(d)) showed that Si phases were

ground evenly along the wear surface without separation. In other words, T6 heat treated alloy is suspected to have achieved greater abrasive wear resistance and lower friction coefficient due to a smaller hardness difference between the matrix and Si phase formed by the reinforcement effects of fine, even Al_2Cu phases (Fig. 1 (b)) from age hardening and improved interface adhesion (Fig. 2(b)) between the Al matrix and Si phase. Al-12wt.% alloy was able to improve wear resistance properties through precipitation hardening (T6) heat treatment, and to maximize its effect, it is necessary to consider the reinforcement of the Al matrix as well as the controlling of interface characteristics between Si phase and matrix.

4. Conclusions

This study investigated the scratch wear properties of Al-12wt.%Si alloy before and after T6 heat treatment using a scratch wear tester, and it obtained the following results:

(1) Despite the grain size slightly increasing after T6 heat treatment, the precipitation hardening effect allowed the T6 alloy to achieve greater hardness properties. The main reinforcement phase was $\theta''(Al_2Cu)$ phase, and θ'' phase is assumed to be dissolved at a solid solution temperature of 510°C and then re-precipitated finely and evenly during aging.

(2) The wear resistance properties evaluated using worn out volume were greater in T6 alloy. In F alloy, the soft matrix characteristic weakened the reinforcement performance of the eutectic Si phase and caused it to easily be dislocated. Meanwhile, the effect of precipitation hardening of θ'' phase at the matrix of T6 alloy was confirmed to be an effective reinforcement phase in wear environments as it allowed the Si phase and matrix to be worn together.

Acknowledgments

This research was supported by Dual Use Technology Program from Republic of Korea.

REFERENCES

[1] A.K. Gupta, B.K. Prasad, R.K. Pajnoo, S. Das, Trans. Nonferrous Met. Soc. China **22**, 1041 (2012).
[2] V.C. Srivastava, R.K. Mandal, S.N. Ojha, Mater. Sci. Eng. A **304**, 555 (2001).
[3] N. Sahib, T. Laoui, A.R. Daud, M. Harun, S. Radiman, R. Yahaya, Wear **249**, 656 (2001).
[4] L. Fang, Y. Fuxiao, Z. Dazhi, Z. Liang, Mater. Sci. Eng. A **528**, 3786 (2011).
[5] M. Zhu, Z. Jian, G. Yang, Y. Zhou, Mater. Design **36**, 243 (2012).
[6] R.X. Li, R.D. Li, Y.H. Zhao, L.Z. He, C.X. Li, H.R. Guan, Z.Q. Hu, Materials Letters **58**, 2096 (2004).
[7] G.S. Ham, M.S. Baek, J.H. Kim, S.W. Lee, K.A. Lee, Met. Mater. Int. **23**, 35 (2017).
[8] S.H. Yoon, S.K. Kim, C.H. Lee, Journal of KWJS **25**, 250 (2007).
[9] A. Amanov, S. Sasaki, D. Kim, O. Penkov, Y.S. Pyun, Tribol. Int. **64**, 24 (2013).
[10] K. Friedrich, H.J. Sue, P. Liu, A.A. Almajid, Tribol. Int. **44**, 1032 (2011).
[11] J.V. Stebut, R. Rezakhanlou, K. Anoun, H. Michel, M. Gantois, Thin Solid Films **181**, 555 (1989).
[12] N. Maan, A. Groenou, Wear, **42**, 365 (1977).
[13] S.K. Sinha, S.U. Reddy, M. Gupta, Tribol. Int. **39**, 184 (2006).
[14] J.I. Weon, Polymer Science and Technology **20**, 265 (2009).
[15] M. Bermudez, W. Brostow, F. Crrion-Vilches, J. Cervantes, G. Damerla, J. Perez, e-Polymers **5**, 22 (2005).
[16] H.J. Kim and C.G. Kim, Journal of the Korean Foundrymens Society **20**, 91(2000).
[17] H.A.H. Steen, A. Hellawell, Acta Metal. Mater. **20**, 363 (1972).
[18] N. Chawla, U. Habel, Y.L. Shen, C. Andres, J.W. Jones, J.E. Allison, Metall. Mater. Trans. A, **31A**, 531 (2000).